JOURNAL OF GUIDANCE, CONTROL, AND DYNAMICS
Vol. 15, No. 3, May-June 1992

Analyzing the Flared Landing Task with Pitch-Rate Flight Control Systems

Ronald A. Hess* and Marduke Yousefpor†
University of California, Davis, Davis, California 95616

A closed-loop handling qualities methodology is applied to an analysis of the flared landing task with pitch-rate flight control systems. A model of pilot behavior throughout approach and flare is developed that postulates the manner in which the pilot may move from pitch attitude to flight-path angle control. Twenty-five configurations flight tested on the NC-131H total in-flight simulator aircraft are analyzed using a structural pilot model and a handling qualities methodology previously reported in the literature. Closed-loop simulation of the simplified landing task is undertaken using the structural model. The pilot ratings from flight test extended the data base supporting the utility of a model-based handling qualities metric. A handling qualities sensitivity function is introduced that may have potential as a design tool.

Introduction

THE economic benefits associated with operating transport aircraft with reduced or "relaxed" longitudinal static stability (improved fuel economy/increased range) are ushering in an era in which designs exhibiting relatively small or even negative static margins are becoming commonplace. The necessity of providing artificial stability augmentation for such aircraft is obvious, and pitch rate command/attitude hold systems appear to be likely choices for fulfilling this role.[1,2] The flight test and analytical research summarized in Ref. 2 clearly demonstrate the problems associated with pitch-rate command stability augmentation systems in the landing flare. One of the recommendations of Ref. 2 was the development of "improved conceptual models of the role of the pilot in the landing task, together with design criteria specifically directed at flying qualities for landing." The work reported summarizes a research effort directed toward the development of such models and criteria.

The research to be described herein involves a pilot/vehicle analysis and simplified computer simulation of the landing flare maneuver using the configurations flight tested on the NC-131H total in-flight simulator (TIFS) and reported in Ref. 3. This data also formed the basis of the study of Ref. 2. The pilot model to be used is the structural model of the human pilot[4] as extended to "pursuit" behavior[5] and employing a model-based handling qualities theory.[6] The next section describes the analytical approach to modeling the flare maneuver, including the handling qualities analysis. Following that, the modeling results are discussed, including the introduction of a new handling qualities criterion of general applicability to piloted aircraft. Finally, conclusions are drawn.

Anaytical Approach

Figure 1, from Ref. 7, describes what might be called a classical, series-loop closure, pilot/vehicle system for precision flight-path control. In one form or another, this loop structure has been used by a variety of researchers; see, for example, Refs. 8–10. In some cases, flight-path angle takes the place of altitude in the outer loop; see for example, Ref. 9. Because of pilot comments regarding a shift of control strategy away from controlling pitch attitude toward controlling flight-path angle in the transition from landing approach to flare, there has been some conjecture as to whether the series-loop structure is a valid one for analyzing the flare maneuver.[11]

Figure 2, adapted from Ref. 11, shows three parts of the landing task, wherein the first and last, respectively, emphasize pitch attitude and flight-path angle control. Figure 3 shows two control loop structures, compensatory (switch in position "0") and pursuit (switch in position "1"), which are intended to model the first and last of these phases, respectively. Both utilize the structural model of the human pilot in which proprioceptive feedback provides the compensation dictated by the crossover model of the human pilot.[4]

A switch has been used in Fig. 3, for simplicity; however, gains that vary from 0 to 1 in complementary fashion can be employed in the pursuit and compensatory paths. The transition could then be explained as a smooth variation in these gains. With the switch in position 0, Fig. 3 is similar to Fig. 1, and compensatory pitch attitude control forms the "primary control loop,"[6] i.e., that loop involving direct manipulative inputs by the pilot. For a visual landing approach using the front-side piloting technique of interest here, rough estimates of minimum attitude and path loop crossover frequencies are 2.0 and 0.5 rad/s, respectively.[12]

A pilot model that may explain the pitch attitude/flight-path angle control strategies just mentioned and provide a path control loop with adequate bandwidth is indicated in Fig. 3 with the switch in position 1. A similar pursuit loop structure has been used to describe higher bandwidth lateral path control activity in near-Earth helicopter maneuvering flight.[5] With the switch in position 1, the pilot has opened the pitch attitude loop but still utilizes the compensation FES/u_1 dictated by the attitude dynamics. Since this compensation obeys the crossover model of the human pilot, the transfer function Θ/Θ_c can be approximated by

$$\frac{\Theta}{\Theta_c} = Ke^{-\tau_e s} \tag{1}$$

over a limited frequency range around crossover. Equation (1) implies that, by adopting the "pursuit" structure of Fig. 3, the pilot can invert the attitude dynamics (with a delay) in the important frequency range around crossover. This inversion has the potential of allowing the pilot to close the outer loop at a considerably higher crossover frequency than is possible with the multiloop compensatory structure of Fig. 3.

Received June 25, 1990; presented as Paper 90-3483 at the AIAA Guidance, Navigation, and Control Conference, Portland, OR, Aug. 20-22, 1990; revision received July 22, 1991; accepted for publication July 29, 1991.

*Professor, Department of Mechanical, Aeronautical, and Materials Engineering. Associate Fellow AIAA.

†Graduate Student, Department of Mechanical, Aeronautical, and Materials Engineering.

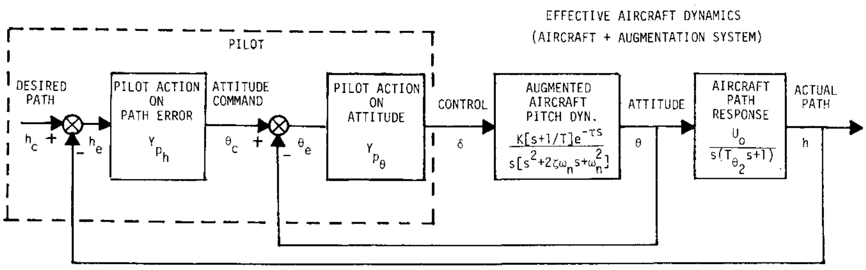

Fig. 1 Classical series-loop closure for flight-path control.

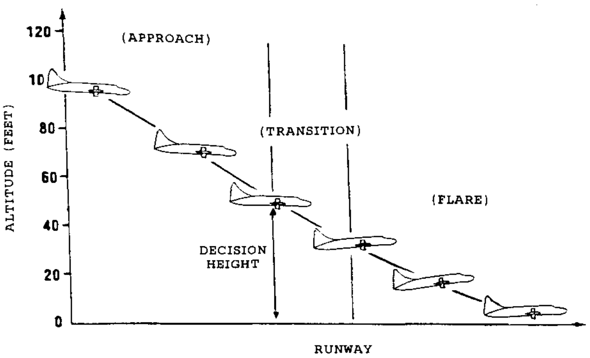

Fig. 2 Parts of the landing task.[11]

Now, the final step in this modeling procedure involves moving the differentiator element s from the pursuit feedforward loop of the structural model to the outer loop and there interpreting $\dot{h}_e$ in terms of flight-path angle error as $\dot{h}_e/U_0$. Figure 4 results. Note that the block with the differentiator s element no longer appears in the pursuit feedforward loop of the structural model. Figures 3 and 4 offer a speculative description of the loop structures in the approach and the flare tasks shown in Fig. 2 and suggest, indirectly, what might occur in the transition phase.

Approach: The loop structure of Fig. 3 is in evidence, with the switch in position 0. Outer altitude control is relatively low bandwidth in nature.

Transition: While retaining the same compensation involved in the closed-loop pitch attitude control of Fig. 3, the pilot begins to open the attitude loop (switch moves from position 0 to 1).

Flare: The loop structure of Fig. 4 is in evidence. Compared with Fig. 3, one sees that altitude rate cues (or, equivalently, flight-path angle) are used in closing the outer loop.

The modeling procedure just outlined can be applied to the test configurations of Ref. 3 as follows:

1) A vehicle/control system configuration is selected from Ref 3.

2) The pitch attitude to control force transfer function Θ/FES is obtained.

3) Based on the characteristics of Θ/FES in the probable region of crossover for compensatory control ($1 < \omega < 5$ rad/s), the basic compensation required of the pilot is determined as if compensatory pitch attitude control was the goal; this means lead, lag, or proportional compensation. This step determines the value of k in the structural model: for lead compensation $k = 2$, for lag compensation $k = 0$, and for proportional compensation $k = 1$.

4) Referring to Table 1, step 3 allows all of the structural model parameters to be selected. In cases of lead or lag compensation, the parameter T_2 is chosen as that required to yield K/s amplitude characteristics in the frequency range of step 3. For the 25 configurations analyzed here, T_2 could be chosen as the reciprocal of the short period undamped natural frequency.

5) Referring to Fig. 4, the compensation Yp_γ is selected to again give K/s-like amplitude characteristics for γ_e/γ with the pitch attitude loop open. For the 25 configurations analyzed here, this step yielded $Yp_\gamma = K_\gamma$.

6) The value of K_γ is chosen to give outer-loop phase and gain margins of at least 45 deg and 4 dB.

7) A computer simulation of the flared landing task is undertaken using the vehicle dynamics and pilot model just discussed. Here, this was accomplished using the computer program ACSL.[13] The flared landing task is simplified in that the flight-path angle command γ_c is generated as a filtered step command given by

$$\gamma_c = 2.5 \cdot \frac{0.5^2}{(s+0.5)^2} \cdot \frac{1}{s} \text{ deg} \tag{2}$$

Equation (2) essentially provides a smooth 2.5-deg change in simulating the transition from the 2.5-deg glide slope to the horizontal runway. No actual touchdown is simulated. The time histories of pertinent variables are recorded. The selection of a second-order filter with a 2-s time constant yields a γ_c, which seemed reasonable for a flare maneuver.

8) For the handling qualities analysis, the methodology of Ref. 6 is employed. This entails, first, moving the compensation element Y_p into the plant and thus creating an "effective plant" Y_c as

$$Y_c = \left(\frac{\gamma}{FES}\right) \cdot (Yp_\gamma) \tag{3}$$

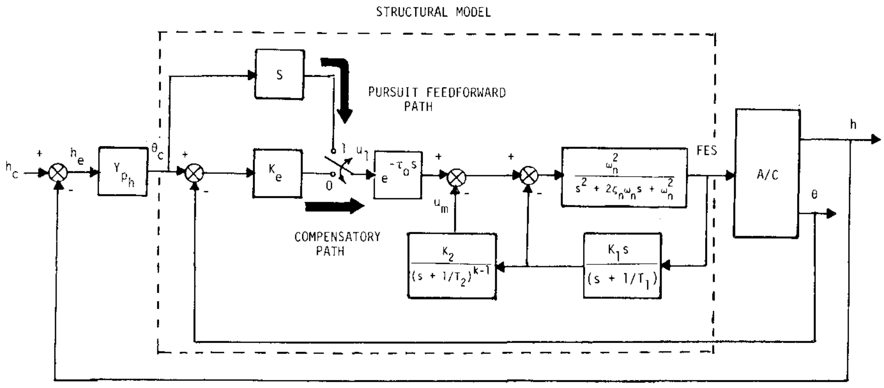

Fig. 3 Structural model for compensatory/pursuit behavior in flight-path control.

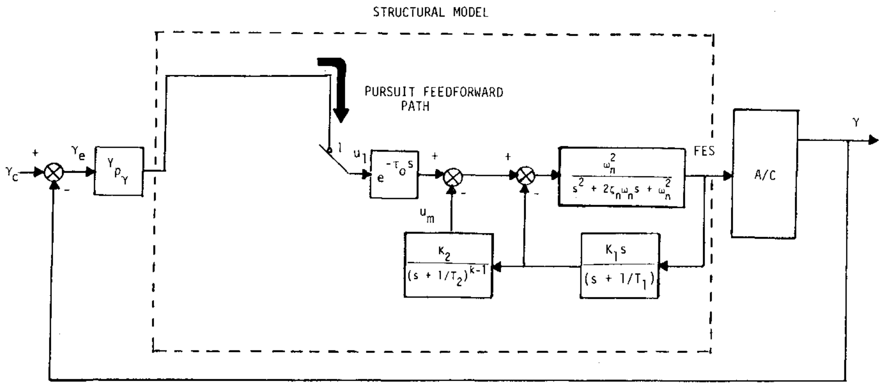

Fig. 4 Structural model for the flared landing task.

This step made the structure of Fig. 4 equivalent to that used in Ref. 6, wherein a compensatory, as opposed to a pursuit, structure was employed and where the gain in the forward loop before the time delay element $e^{-\tau_0 s}$ was unity.

Second, as discussed in Ref. 6, the mean square value of u_m is calculated in simulation for the configurations under study at a common crossover frequency. This value was chosen here as 0.4 rad/s. The common crossover frequency is simply an efficient and expedient means of transforming task performance requirements (as interpreted by the analyst) into a variable that is compatible with the model formulation with the goal of assessing vehicle handling qualities. The 0.4 rad/s value here is felt to be representative of a lower limit for this task and resulted in a stable pilot/vehicle system for all of the configurations analyzed. As discussed in Ref. 6, the variable u_m is proportional to vehicle output rate due to control activity, and the value of σ^2_{um} so obtained through the procedure just outlined has been shown to correlate with pilot handling qualities ratings (HQRs) from a number of experiments.

Table 1 Nominal parameters for structural model

k	K_v	K_1	K_2	T_1,s	T_2,s	τ_0,s	ζ_n	ω_n, rad/s
0	0	1.0	2.0	5.0	—[a]	0.15	0.707	10.0
1	0	1.0	2.0	5.0	—[b]	0.15	0.707	10.0
2	0	1.0	10.0	2.5	—[a]	0.15	0.707	10.0

[a]Selected to achieve K/s-like crossover characteristics.
[b]Parameter not applicable.

Results

Table 2 and Fig. 5 show the characteristics of the configurations flight-tested on the TIFS that were analyzed here. In the study of Ref. 3, the gains K_α, K_L, K_q, and K_I and the aircraft model were selected to produce desired vehicle response characteristics. In terms of Fig. 5, the transfer function Θ/δ_1 was

$$\frac{\Theta}{\delta_1} \simeq \frac{K_\Theta(s + K_I)[s + (1/T_{\Theta 2})]}{s(s + \lambda_2')\,(s^2 + 2\zeta_{sp}\omega_{sp}s + \omega_{sp}^2)} \tag{4}$$

Figures 6 and 7 show typical model simulation results for a pair of configurations from Ref. 3. Each of the figures show stick force FES, flight-path angle γ, pitch attitude Θ, and altitude h for a simulated flare. It should be noted that the graphs depict changes from the equilibrium condition on a −2.5-deg glide slope, so the flare appears as a climb in the figures. Figure 6 shows results for configuration 1-2-2 from Ref. 3, whereas Fig. 7 shows configuration 4-2-2 with dynamics identical to those of 1-2-2, but with a lead/lag filter shaping the control stick output.

Table 2 Configuration definitions

Configuration	$\omega_{n_{sp}}$	ζ_{sp}	$1/T_{\Theta 2}$	λ_2'	K_I	T_Z	T_F	$1/T_{wo}$	τ
1-1-1	2.79	0.8	0.38	0.44	2	0	0	0	0
1-2-2	2.76	0.8	0.72	0.82	2	0	0	0	0
1-3-7	2.73	0.8	1.0	1.19	2	0	0	0	0
2-1-1	1.78	0.6	0.38	0.5	2	0	0	0	0
2-2-2	1.75	0.6	0.72	0.93	2	0	0	0	0
3-1-3	(0.4)[a]	—	0.38	0.25	0	0	0	0	0
3-2-4	(0.4)	—	0.72	0.25	0	0	0	0	0
4-1-1	2.79	0.8	0.38	0.44	2	2.3	0.5	0	0
4-2-2	2.76	0.8	0.72	0.82	2	1.22	0.5	0	0
4-3-7-1	2.73	0.8	1.0	1.19	2	0.84	0.5	0.2	0
5-1-1	1.78	0.6	0.38	0.5	2	2.0	0.5	0	0
5-2-2	1.75	0.6	0.72	0.93	2	1.07	0.5	0	0
6-1-1	2.27	0.46	0.38	0.45	3	0	0	0	0
6-1-1-1	2.27	0.46	0.38	0.45	3	0	0	0.2	0
6-2-1	2.27	0.46	0.38	0.45	3	2.23	0.33	0	0
6-2-1-1	2.27	0.46	0.38	0.45	3	2.23	0.33	0.2	0
7-1-4	2.84 (0.16)[b]	0.8 (0.01)	0.72	—	0	0	0	0	0
8-1-5	1.45	0.5	0.4	0.586	2	1.67	0.5	0	0
8-1-5-1	1.45	0.5	0.4	0.586	2	1.67	0.5	0.2	0
8-2-5	1.09	0.5	0.4	0.7	2	1.0	0.5	0	0
8-3-5	1.45	0.5	0.4	0.586	2	0.667	0.5	0	0.047
8-3-5-1	1.45	0.5	0.4	0.586	2	0.667	0.5	0.2	0.047
8-4-6	1.47	0.6	0.4	0.590	2	1.67	0.5	0	0
8-5-5	1.45	0.5	0.4	0.586	2	1.67	0.5	0	0.035
8-5-5-1	1.45	0.5	0.4	0.586	2	1.67	0.5	0.2	0.035

[a]Short period roots replaced by first-order pole at $s = -(\ )$.
[b]Phugoid mode.

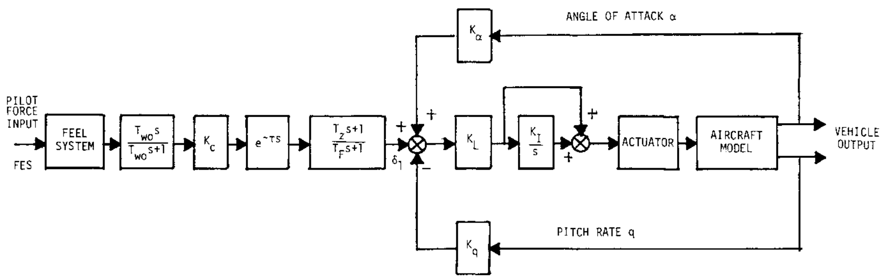

Fig. 5 TIFS flight control system.

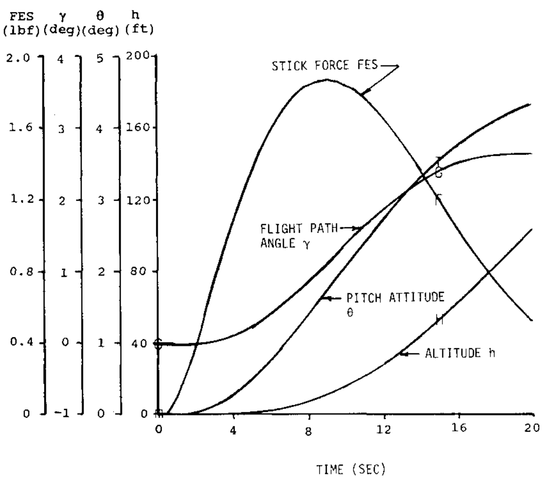

Fig. 6 Closed-loop simulation of landing flare for configuration 1-2-2.

It is interesting to note that the objectionable "push to land" control input characteristics that pilots often find objectionable in pitch command flight control systems[1-3] are evident in the simulations of configurations 1-2-2 and 4-2-2. Note the different scales on the control force ordinate in Figs. 6 and 7. Although the stick force does not change in sign, the reduction in "pull" evident in Figs. 6 and 7 would represent a forward stick motion during the latter part of the flare maneuver. An examination of the stick force time history in the simulation of a configuration with conventional pitch attitude dynamics (configuration 7-1-4) revealed little reduction in pull.

The flight-path angle response of configuration 4-2-2 is seen to exhibit a smaller time constant than that of configuration 1-2-2. This is attributable to the fact that, in following step 6 in the preceding section, the crossover frequency of configuration 4-2-2 was 0.59 rad/s, whereas configuration 1-2-2 was only 0.2 rad/s.

Figure 8 shows the values of σ_{um}^2 plotted on the data from Ref. 6. In generating σ_{um}^2, flight-path angle was expressed in degrees. The slope of the steeper portion hand-faired straight line in Fig. 8 has been modified from that appearing in Ref. 6 to better reflect the data trends. In addition, the bounds on the steeper portion have been increased to ± 1.5 HQRs. An examination of Fig. 8 shows that 78% of the data falls within the dashed lines, and this data now includes experiments from 5 diverse data sources involving simulation/flight-test results from 58 different configurations/tasks.

It is difficult to clearly indicate the handling qualities rating variation between the two evaluation pilots in Fig. 8. However, Fig. 9, from Ref. 3, does this for those configurations that both pilots evaluated (68% of the configurations analyzed here). As can be seen in Fig. 9, there is considerable variation from the line of agreement in the flight test results.

The correlation between σ_{um}^2 and HQRs shown in Fig. 8 is somewhat poorer than the correlation between flight-path angle peak overshoot and HQRs obtained by Berry[14] and comparable to the correlation between altitude bandwidth and HQRs obtained by Sarrafian and Powers.[10] However, these metrics were developed specifically for the landing flare task using the data of Ref. 3, whereas the metric discussed in Ref. 6 and used here is, theoretically, applicable to any flight task. Nonetheless, using Fig. 8 for prediction of HQRs for the landing flare would be problematic.

Figure 10 is a comparison of HQRs and model results (σ_{um}^2) for configurations showing the effect of the addition of lead/lag and washout prefilters in the flight control system. The data selected for inclusion in Fig. 10 were those in which at least two pilot ratings were obtained for each configuration in flight test. Note that configurations 1-2-2 and 4-2-2 from Figs. 6 and 7 are included in Fig. 10.

Handling Qualities Sensitivity Function

It is of obvious interest to determine why some simulated pilot/vehicle configurations result in larger σ_{um}^2 (and poorer HQRs) than others in this study. Since σ_{um}^2 is the metric in question and since

$$\sigma_{um}^2 = \frac{1}{2\pi}\int_{-\infty}^{+\infty} \left|\frac{u_m(j\omega)}{\gamma_c(j\omega)}\right|^2 \cdot \Phi_{\gamma_c\gamma_c}(\omega)\,d\omega \qquad (5)$$

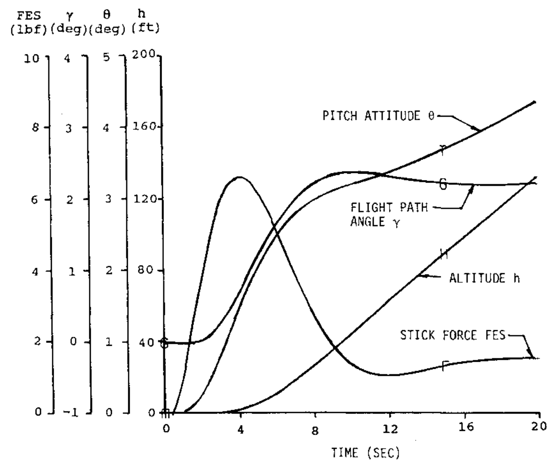

Fig. 7 Closed-loop simulation of landing flare for configuration 4-2-2.

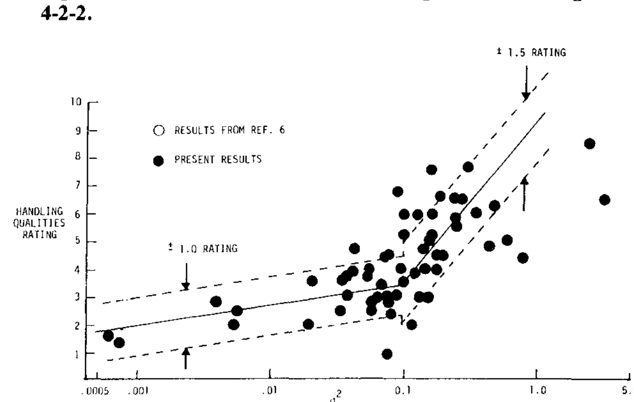

Fig. 8 Handling qualities ratings vs mean square value of u_m.

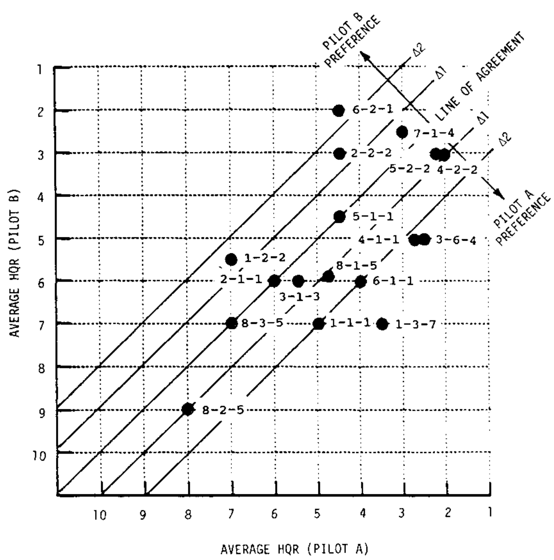

Fig. 9 Pilot rating variations from Ref. 3.

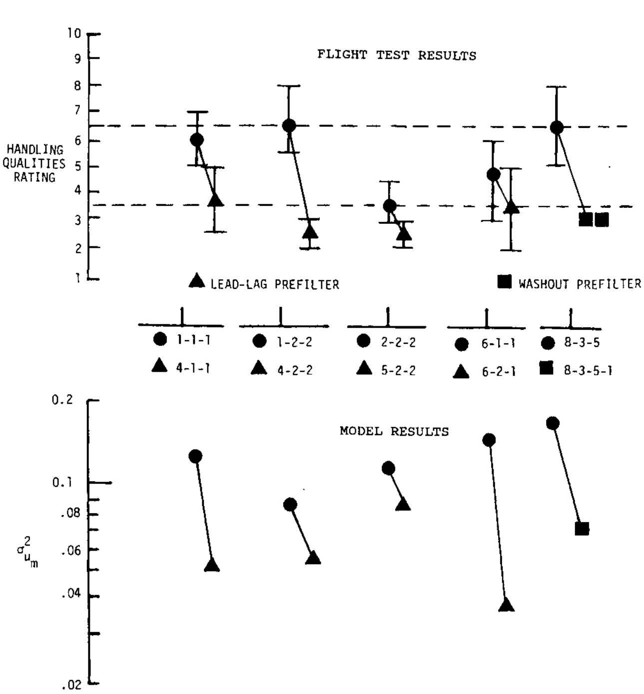

Fig. 10 Flight test and model results for a series of configurations.

an examination of $|u_m(j\omega)/\gamma_c(j\omega)|$ was undertaken for a number of configurations, both in this study and those used in Ref. 6. To encompass tasks for which variables other than flight-path angle served as the command input, the transfer function in question will be denoted u_m/c and referred to as the handling qualities sensitivity function. The term "sensitivity function" was chosen since it can be shown that u_m/c is similar in appearance to the error-to-input transfer function in the pilot/vehicle system, e.g., γ_e/γ_c in Fig. 4. This latter transfer function is often referred to as the sensitivity function in the control systems literature.[15]

Figure 11 shows the energy spectral density of u_m for configurations 2-1-1 and 4-2-2, which received average HQRs of 6.0 and 2.5, respectively, in the study of Ref. 3. Note that the area under the curve for configuration 2-1-1 is considerably larger than that for 4-2-2, and so, by Eq. (5), σ^2_{um} will be considerably larger for the former. Figure 12 shows the magnitude portion of the Bode plots for u_m/γ_c for these configurations. Note that the curve for 2-1-1 is greater than unity around the 0.4 rad/s crossover frequency. It is this characteristic that leads to the larger σ^2_{um} value for this configuration. The region of crossover is the critical region, since at lower frequencies $|u_m(j\omega)/\gamma_c(j\omega)|$ is small due to the effect of feedback, and at higher frequencies there is little power in the input γ_c.

Figure 13 compares the sensitivity functions for configurations 8-2-5 and 7-1-4, which received average HQRs of 7.5 and 2.8, respectively. Recall that 7-1-4 represented a conventional aircraft. The configuration definitions are shown in Table 2. Configuration 8-2-5 is described as an alternate Shuttle flight control system.[3] Figure 13 shows the amplitude peak of the sensitivity function for configuration 8-2-5 exceeding unity in a frequency range approximately one-half decade above the 0.4 rad/s crossover frequency used in the handling qualities analysis.

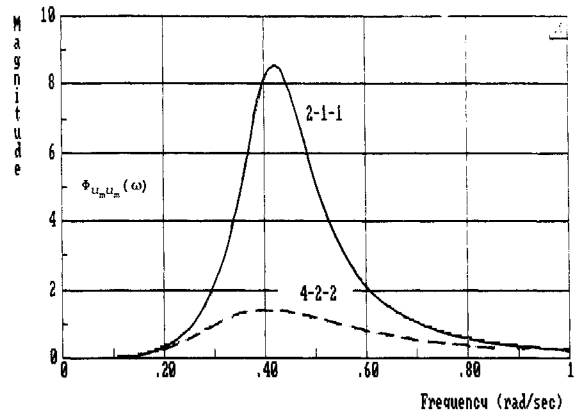

Fig. 11 Energy spectral density of u_m for configurations 2-1-1 and 4-2-2.

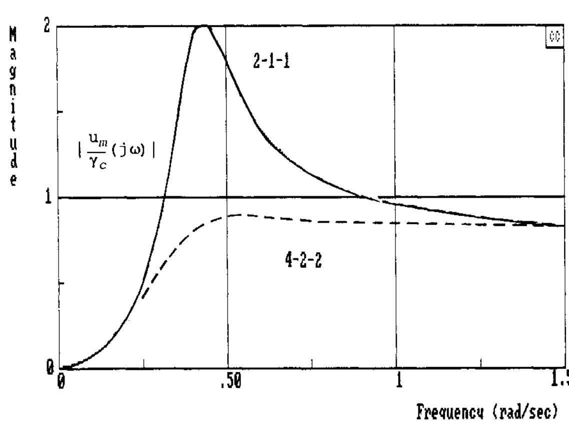

Fig. 12 Handling qualities sensitivity functions for configurations 2-1-1 and 4-2-2.

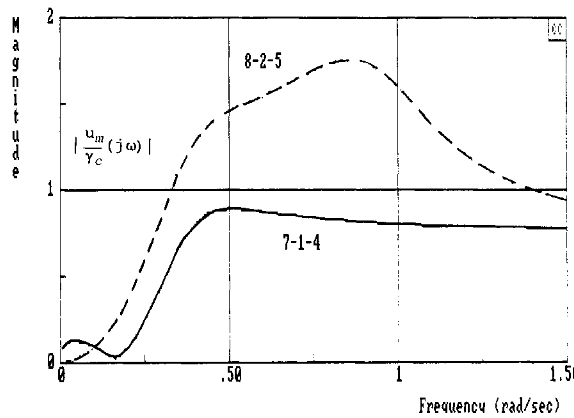

Fig. 13 Handling qualities sensitivity functions for configurations 8-2-5 and 7-1-4.

The ability of the sensitivity function to discriminate between flight control systems that received HQRs differing by as much as 4.75 units on the Cooper-Harper scale is not, in itself, an impressive accomplishment. Figure 14 shows the sensitivity functions associated with an application of the handling qualities methodology to configurations 2-2-2 and 5-2-2 that received average HQRs of 3.8 and 2.5, respectively. As can be seen, the sensitivity functions discriminate between the "solid" level 1 configuration and the configuration just within level 2. Note that, although the sensitivity function for 5-2-2 does exceed unity, it does so at frequencies well above the 0.4 rad/s crossover frequency where there is little power in γ_c.

In examining a number of the configurations from those analyzed in Ref. 6, a pattern consistent with that just described was found. Specifically, if the magnitude of the handling qualities sensitivity function exceeded unity around the open-loop crossover frequency, the configuration was rated as level 2 or 3 by the evaluation pilot(s). Conversely, if the magnitude of the sensitivity function did not exceed unity around the open-loop crossover frequency, the configuration was rated as level 1 by the evaluation pilot(s). This pattern was consistent for the cases examined across vehicle configurations and tasks for the range of vehicles and tasks examined in Ref. 6.

Using the sensitivity function as a means of delineating level 1 from level 2-3 HQRs in the 25 configurations analyzed here resulted in an 80% success rate. Of the five configurations that were incorrectly classified by the sensitivity function, four were classified as level 1, which actually received average HQRs of level 2. However, the average of these level 2 ratings was 4.0, i.e., within an average 0.5 HQR of the 3.5 rating separating level 1 from level 2. Finally, even in those cases in which the sensitivity function incorrectly classified configurations, it identified improvement. Consider Fig. 15, which compares the sensitivity functions for configurations 8-3-5 and 8-3-5-1, which differ only in the use of a washout prefilter on control stick inputs in the latter. The average HQRs that the pilots gave for these configurations were 6.7 (8-3-5) and 3.0 (8-3-5-1). Note that, although the sensitivity function for 8-3-5-1 does not correctly classify this configuration as level 1, it does correctly indicate a rating improvement over 8-3-5. Of course, this fact is also indicated in the σ^2_{um} values of Fig. 10.

The apparent ability of the sensitivity function to reflect handling qualities in a relatively simple fashion suggests that it has the potential to be used as a design tool by the flight control systems/handling qualities engineer. The design dictum would simply be the following: Tailor the vehicle dynamics in the task at hand so that the amplitude of the handling qualities sensitivity function remains at or below unity for frequencies around the open-loop crossover. This process would be iterative in nature, since changes in the vehicle dynamics can produce changes in the pilot model parameters of Table 1. The crossover frequency remains as the one parameter that the analyst must choose in exercising the proposed handling qualities technique.

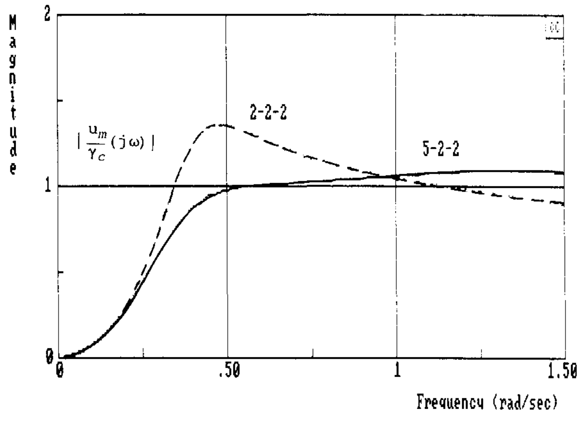

Fig. 14 Handling qualities sensitivity functions for configurations 2-2-2 and 5-2-2.

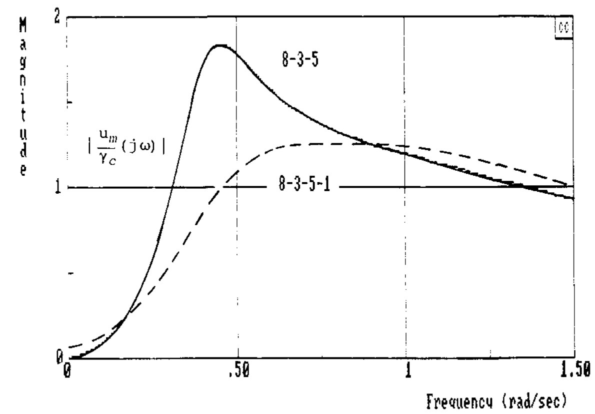

Fig. 15 Handling qualities sensitivity functions for configurations 8-3-5 and 8-3-5-1.

At this juncture, it is worth repeating two important points in applying the handling qualities methodology of Ref. 6.

1) The first part of step 8 in the preceding section is a necessary part of the procedure, i.e., forming an effective plant by moving the compensation Yp_γ into the original plant.

2) Control system sensitivity effects are not included in the analysis.

Conclusions

The goal of developing an improved conceptual model of the role of the pilot in the landing task has been approached using a pilot model that has proved effective in other studies, namely, a structural model of the human pilot. By employing the structural model with compensatory and pursuit modes, a model of pilot behavior throughout approach and flare has been developed that postulates the manner in which the pilot may move from pitch attitude to flight-path angle control. Exercising the model in a closed-loop simulation of the landing flare produced time histories that reflected one of the shortcomings of pitch command flight control systems, namely, the necessity of providing forward stick motion in flare. A handling qualities methodology applied to 25 vehicle configurations simulated on the TIFS aircraft extended the data base supporting the utility of a metric based on the mean square value of the variable u_m in the structural model. This variable is proportional to vehicle output rate due to control activity. Finally, a handling qualities sensitivity function was proposed that has the potential of being used as a design tool for the control systems/handling qualities engineer. In exercising a handling qualities criterion based on the sensitivity function for the TIFS data to delineate level 1 from level 2-3 handling qualities, an 80% success rate was achieved.

Acknowledgment

This research was supported by Grant NAG 2-490 from NASA Ames Research Center, Dryden Flight Research Facility. Donald T. Berry was the contract technical manager.

References

[1]Mooij, H. A., and van Gool, M. F. C., "Flight Test of Stick Force Stability in Attitude-Stabilized Aircraft," *Journal of Aircraft*, Vol. 15, No. 9, 1978, pp. 562-566.

[2]Chalk, C. R., "Flying Qualities of Pitch Rate Command/Attitude Hold Control Systems for Landing," *Journal of Guidance, Control, and Dynamics*, Vol. 9, No. 5, 1986, pp. 541-545.

[3]Berthe, C. J., Chalk, C. R., and Sarrafian, S., "Pitch Rate Flight Control Systems in the Flared Landing Task and Design Criteria Development," NASA CR-172491, Oct. 1984.

[4]Hess, R. A., "A Model-Based Theory for Analyzing Human Control Behavior," *Advances in Man-Machine Systems Research*, Vol. 2,

edited by W. B. Rouse, JAI Press, Greenwich, CT, 1985, pp. 129–175.

[5]Hess, R. A., and Chan, K. K., "A Preview Control Pilot Model for Near-Earth Maneuvering Helicopter Flight," *Journal of Guidance, Control, and Dynamics,* Vol. 11, No. 2, 1988, pp. 146–152.

[6]Hess, R. A., "Theory for Aircraft Handling Qualities Based Upon a Structural Pilot Model," *Journal of Guidance, Control, and Dynamics,* Vol. 12, No. 6, 1989, pp. 792–797.

[7]McRuer, D., and Myers, T. T., "Flying Qualities of Relaxed Static Stability Aircraft," Vol. II, Final Report, Department of Transportation, DOT/FAA/CT-82/130 II, Sept. 1982.

[8]Hess, R. A., and Watson, D. C., "Cross Coupling in Pilot-Vehicle Systems," *Journal of Guidance, Control, and Dynamics,* Vol. 9, No. 2, 1986, pp. 614–620.

[9]Anderson, M. R., and Schmidt, D. K., "Closed-Loop Pilot Vehicle Analysis of the Approach and Landing Task," *Journal of Guidance, Control, and Dynamics,* Vol. 10, No. 2, 1987, pp. 187–194.

[10]Sarrafian, S. K., and Powers, B. G., "Application of Frequency-Domain Handling Qualities Criteria to the Longitudinal Landing Task," *Journal of Guidance, Control, and Dynamics,* Vol. 11, No. 4, 1988, pp. 291–293.

[11]Martz, J. J., Biezad, D. J., DiDominico, E. D., "Loop Separation Parameter: A New Metric for Landing Flying Qualities," *Journal of Guidance, Control, and Dynamics,* Vol. 11, No. 6, 1988, pp. 535–541.

[12]Ashkenas, I. L., "Twenty-Five Years of Handling Qualities Research," *Journal of Aircraft,* Vol. 21, No. 5, 1984, pp. 289–301.

[13]Anon., "Advanced Continuous Simulation Language (ACSL)," User Guide/Reference Manual, Mitchell and Gauthier Assoc., Concord, MA, 1981.

[14]Berry, D. T., "A Flight-Path-Overshoot Flying Qualities Metric for the Landing Task," *Journal of Guidance, Control, and Dynamics,* Vol. 9, No. 6, 1989, pp. 609–613.

[15]Maciejowski, J. M., *Multivariable Feedback Design,* Addison Wesley, New York, 1989.